Effect of heat shock on ultrastructure and calcium distribution in Lavandula pinnata L. glandular trichomes.

By: S.S. Huang, Bruce K. Kirchoff and J.P. Liao

Abstract:

The effects of heat shock (HS) on the ultrastructure and calcium distribution of *Lavandula pinnata* secretory trichomes are examined using transmission electron microscopy and potassium antimonate precipitation. After 48-h HS at 40°C, plastids become distorted and lack stroma and osmiophilic deposits, the cristae of the mitochondria become indistinct, the endoplasmic reticulum acquires a chain-like appearance with ribosomes prominently attached to the lamellae, and the plasma and organelle membranes become distorted. Heat shock is associated with a decrease in calcium precipitates in the trichomes, while the number of precipitates increases in the mesophyll cells. Prolonged exposure to elevated calcium levels may be toxic to the mesophyll cells, while the lack of calcium in the glands cell may deprive them of the normal protective advantages of elevated calcium levels. The inequality in calcium distribution may result not only from uptake from the transpiration stream, but also from redistribution of calcium from the trichomes to the mesophyll cells.

Keywords: plant sciences | cell biology | zoology | lavandula pinnata L | glandular trichomes | heat shock | calcium | antimonite precipitates | ultrastructure

Article:

Introduction

As a common environmental stress in plants, heat shock (HS) is a major constraint on vegetative growth (Wahid et al. *2007*; Abdelmageed and Grudaz *2007*). Responses to HS, such as cellular damage and the disruption of physiological metabolism, have been well documented (Vierling *1991*; Blum *1996*; Wang et al.*1997*). For instance, prominent ultrastructural changes in the nucleus, endoplasmic reticulum (ER), mitochondria, plastids, and plasma membranes have been reported to accompany HS (Ciamporova and Mistrik *1993*; Collins et al. *1995*). In maize

root cells, HS reduces the density of mitochondria, decreases the number of cristae, and is associated with an accumulation of electron dense inclusions in the cytoplasm (Ciamporova and Mistrik *1993*).

The calcium ion (Ca^{2+}), a common second messenger, has been implicated in the regulation of plant responses to environmental stress (Simon *1978*; Bush *1995*; Webb et al. *1996*). A number of studies have found that Ca^{2+} distribution and levels change in response to environmental stress (Gilroy et al. *1990*; Palta*1990*; Gong et al. *1998*; Zhao and Tan *2005*). Stresses such as physical contact, cold shock, fungal elicitors, and HS lead to a rapid increase in Ca^{2+} concentration ($[Ca^{2+}]$) in the cytoplasm (Knight et al. *1991*). Following HS, increased intracellular $[Ca^{2+}]$ has been found in pea mesophyll protoplasts (Biyaseheva et al. *1993*), tomato fruits (Starck et al. *1994*), anthers (Yan et al. *2002*), and pear cells (Klein and Ferguson *1987*). The increase in $[Ca^{2+}]$ initiates gene expression, triggers cascades of biochemical events, maintains cell cycle progression (Clapham *1995*), and increases a plant's tolerance to HS (Gong et al. *1998*). Pretreatment with chemicals that reduce intercellular $[Ca^{2+}]$, such as the Ca^{2+} chelator ethylene glycol-bis (2-aminoethyl ether)-N, N, N′, N′-tetraacetic acid (EGTA), or the plasma membrane Ca^{2+} channel blockers La^{3+} and verapamil, reduces a plant's intrinsic heat tolerance (Gong et al. *1997*; Zhang et al. *2000*). However, excessive $[Ca^{2+}]$ can also be cytotoxic (Hepler and Wayne *1985*; Biyaseheva et al. *1993*; Wang and Li *1999*). Prolonged high $[Ca^{2+}]$ are associated with the degradative processes of programmed cell death—apoptosis, cleaving DNA, and degrading cell chromatin (Nicotera et al. *1994*; Clapham *1995*; Boursiac et al. *2010*).

Plants acquire Ca^{2+} primarily in solution from the soil and transport it to the shoot via the xylem (White *2001*). In leaves, mineral ions move by bulk flow in the transpiration stream (Leigh and Tomos *1993*; Karley et al.*2000*). Fluorescent dyes fed to cereal leaves via the xylem reach leaf epidermal cells through vein extension pathways and appear to bypass the mesophyll cells (Canny *1990*). These results lead one to believe that Ca^{2+} moves along the same path. However, the route of calcium transport during HS has never been fully elucidated. All that is known is that HS results in an increase in intracellular $[Ca^{2+}]$, which arises largely from extracellular sources (Gong et al. *1998*).

Although the response of plant leaves and anthers to heat shock has been widely investigated (Gong et al.*1997*; Zhang et al. *2000*; Yan et al. *2002*), little is known about how HS affects the development of glandular trichomes. Neither is it clear how HS interacts with calcium distribution during glandular trichome development.

In our previous papers, we described the ultrastructure of the glandular trichomes of *Lavandula pinnata* L. and calcium distribution in these trichomes (Huang et al. *2008*, *2010*). This species possesses two types of secretory trichomes: one- to two-celled capitate and eight-celled spherical trichomes that are called "peltate" because of their structure in other Lamiaceae (Amelunxen and Gronau *1968*; Antunes and Sevinate-Pinto*1991*; Werker *1993*; Turner et al. *2000*;

Gersbach *2002*). Capitate trichomes secrete mainly lipophilic and polysaccharidic substances, while the peltate trichomes only secrete lipophilic substances (Werker *1993*).

During normal trichome development, the distribution of loosely bound calcium changes dynamically (Huang et al. *2010*). In the early stages of gland development, loosely bound calcium is found on the cell walls, plasma membrane, and tonoplast. As the trichomes approach maturity, calcium becomes more abundant in the subcuticular space (SCS) adjacent to the external cell walls but is depleted in the stalk and basal cells and especially in the cytoplasm and vacuoles of the apical cells. Finally, at the post-secretory stage, calcium levels decrease in the SCS, and calcium becomes irregularly distributed in the apical cell cytoplasm (Huang et al. *2010*). Experiments with the calcium channel blocker nifedipine and the calcium chelator EGTA show that normal trichome development and secretion are calcium dependent (Huang et al. *2010*).

The present study was designed to investigate loosely bound calcium distribution in the glandular trichomes of *L. pinnata* following HS. We expected calcium to increase following HS, while a prolonged exposure to HS is expected to lead to calcium levels that are toxic to the cells. Prolonged exposure to HS is also expected to lead to a decrease in secretory product. To test these hypotheses, leaves of *Lavandula* were treated with different durations of HS, and the loosely bound calcium was visualized with potassium antimonate precipitation. Calcium levels in spongy mesophyll cells and vascular bundles were also measured in order to elucidate the route of calcium transportation under HS.

Materials and methods

Controls

Procedures for the study of trichome development and mesophyll structure without antimonate are reported in Huang et al. (*2008*). Procedures and controls for studying calcium visualization, including light-grown controls, dark-grown controls, treatment with 100 mM Nif, and treatment with 5 mM EGTA are reported in Huang et al. (*2010*). Precipitates were confirmed as calcium antimonate with a JEOL 2000FX TEM equipped with an IXRF energy dispersive X-ray analysis system (Huang et al. *2010*). These controls, and the new experiments reported here, were carried out at the same time.

Calcium distribution following heat shock

Sterilized seeds of *L. pinnata* L. (purchased from Kew Gardens, UK) were germinated on a thin wet layer of cotton in plastic trays inside a growth chamber (24°C, 100 % RH, 11 W m^{-2} light intensity, 16 h daylight). After 5 days, uniformly sized seedlings (1–2 cm) were transferred to small plastic cups containing sand and a complete fertilizer, including calcium. After 10 days, the seedlings were transferred to a second growth chamber to induce HS (40°C, 100 % RH, 11 W m^{-2} light intensity, 16 h daylight). Leaves at different developmental stages (different leaf

lengths) were collected after 0 (control), 12, 24, and 48 h HS (Yan et al. *2002*). One third of the plants treated for 48 h were returned to 24°C for 16 h to allow the plants to recover. All the experiments were done in three replicates (six plants per treatment).

Subcellular calcium localization was visualized according to the method of Slocum and Roux (*1982*), with minor modifications. Leaves were cut into approximately 1-mm^2 pieces and fixed in 2 % glutaraldehyde in 0.1 M potassium phosphate (KH_2PO_4) buffer (pH 7.8) containing 1% potassium antimonate ($K_2H_2Sb_2O_7 \cdot 4H_2O$). Fixation was carried out for 4 h at 4°C. The fixed pieces were then washed in three changes of 1% potassium antimonate in 0.1 M potassium phosphate buffer (0.5 h each) and post-fixed in 1 % osmium tetroxide (OsO_4) for 16 h at 4°C in the same potassium antimonite–buffer combination. The post-fixed tissues were washed in three changes of 0.1 M potassium phosphate buffer without antimonite, dehydrated in a graded ethanol series, and embedded in Spurr's resin. Ultrathin sections (80 nm) were cut using a Leica Ultracut S ultramicrotome, stained with uranyl acetate and observed with a JEM-1010 transmission electron microscope at 90 kV.

Two additional controls were also used: (1) potassium antimonate was sometimes omitted from the solutions during processing; (2) selected grids with specimens containing calcium precipitates (ppts) were incubated in a solution of 0.1 M EGTA for 1 h at 37°C to remove the ppts (Wick and Hepler *1980*; Tian and Russell *1997*).

The abundance of the calcium precipitates in peltate trichomes was determined by calculating the number of the precipitates per square micrometer on each micrograph. Four to six peltate glandular trichomes were examined at each stage to determine calcium abundance in the various regions or organelles (Table 1). An electron micrograph of a section was selected from each trichome/stage, and the number of ppts in a defined area was counted. The area to be counted was chosen based on the presence of clear ppts but without reference to the specific features of the organelle or region (haphazard sampling). The sizes of the few large ppts (Fig. 2d) that occurred in the samples were determined by estimating the number of small ptts into which they could be decomposed. In the two cases where only four trichomes were found (presecretory stage following 12 and 24 h HS), the number of ppts in two sections from two of the trichomes were sampled, to give six sample points. The sampled values were averaged both within organelles/regions, and across all organelle/regions to produce Fig. 1. In the case of the mesophyll cells, ppt counts in the apoplast were included in the overall average (Fig. 1).

Mesophyll cell			Glandular trichomes					
			Initial cell stage		Presecretory stage		Secretory stage	
N	H		N[a]	H	N[a]	H	N[a]	H

	0 h	12 h	48 h	0 h	12 h	48 h	0 h	12 h	48 h	0 h	12 h	48 h
Cell wall	0	10.00 ±1.81 +	34.67 ±2.19 ++	50.33 ±3.67 +++	7.0 ±1.65+	0	29.33 ±4.33++	6.33 ±1.45+	0	52.00 ±4.49 +++	0	0
Plasma membrane	7.50 ±1.26+	9.00 ± 0.89+	32.00 ±2.58 ++	29.50 ±2.1 1++	7.0 ±0.97+	0	30.00 ±3.60++	10.50 ±1.38+	0	28.17 ±3.66 ++	10.23 ±1.28+	0
Tonoplast	18.33 ±1.63+	11.83 ±1.49 +	6.33 ± 1.26+	32.7 ±2.83++		0	27.00 ±2.48++	5.50 ±0.85+	0	0	0	0
Cytosol	0	32.67 ±2.89 ++	53.67 ±3.83 +++	10.67 ±1.43+	0	0	10.17 ±1.54+	0	0	0	0	0
Nucleus	32.83 ±1.89++	58.0 ± 2.45+	123.33 ±6.88 ++++	32.50 ±3.27++	16.7 ±1.65+	0	28.33 ±2.96++	18.83 ±1.17+	0	0	0+	0
Mitochondria	2.17 ±0.48+	3.83 ± 0.60+	23.0 ± 2.78++	4.00 ±0.58+	2.17 ±0.48+	0	2.00 ±0.26+	1.67 ±0.42+	0	0	0	0
Chloroplast/plastid	22.00 ±2.11++	19.3 ± 1.33+	30.17 ±2.96 ++	5.67 ±0.88+	1.83 ±0.60+	0	1.83 ±0.31+		0	0	1.06 ±0.19+	0
Intercellular spaces	30.00 ±3.60++	29.83 ±3.61 ++	7.00 ± 1.06+	Not applicable								
Vessel elements	23.33 ±2.73++	49.17 ±4.08 +++	65.5 ± 5.25++	Not applicable								
SCS	Not applicable									114.0 ±7.25 ++++	1.17 ±0.31 +	0

Mean ± SE, with assessments of relative abundance. Four to six glandular trichomes were examined at each stage

+ 1–19 precipitates/μm^2 (uncommon), ++ 20–39 precipitates/μm^2 (common), +++ 40–59 precipitates/μm^2 (abundant), ++++ 60 or more precipitates/μm^2 (very abundant), *SCS* subcuticular space

[a] The data on normal (no HS) calcium distribution is from Huang et al. (*2010*)

Figure 1 has been omitted from this formatted document.

Results

Control: gland ultrastructure during normal growth

The results presented here are a summary of Huang et al. (*2008*). Four stages of gland development and secretion have been recognized: the gland initial cell before any cell divisions have occurred, the presecretory stage, the secretory stage, and the post-secretory stage (Huang et al. *2008*). The presecretory stage includes all developmental phases from the first division of the initial cell to the inception of gland filling. The secretory stage commences with the beginning of gland filling and the consequent separation of the thickened cuticle from the cell walls. Post-secretory stage glands have filled SCS and appear as spherical domes inserted in slight depressions in the leaf epidermis.

At glandular trichome initiation, the initial cells appear meristematic and have few small vacuoles, relatively large nuclei, large nucleoli, numerous ribosomes, and many mitochondria and proplastids (Huang et al. *2008*, their Fig. 2A). The basal portions of the cells are vacuolated, while the apical portions are cytoplasmically dense (Huang et al. *2008*, their Fig. 2A). In the capitate trichomes at the presecretory stage, the apical cells have abundant proplastids, Golgi, and short cisternae of rough endoplasmic reticulum (RER). Small, granulose (starch) and osmiophilic deposits (lipids) appear in the proplastids (Huang et al. *2008*, their Fig. 3A). At the secretory stage, lipid droplets and Golgi bodies are more abundant than at earlier stages. RER are found appressed to, and vesicles with osmiophilic substances are tightly associated with, the plasma membrane, suggesting exocytosis (Huang et al. *2008*, their Fig. 4E). As secretion continues, the cuticle begins to separate from the cell wall to form a SCS, which gradually fills with secretory product. At this stage, RER are still abundant, as are osmiophilic substances in the plastids (Huang et al. *2008*, their Fig. 4F). During the post-secretory stage, the SCS is full of lipophilic secretory product (Huang et al. *2008*, their Fig. 4G).
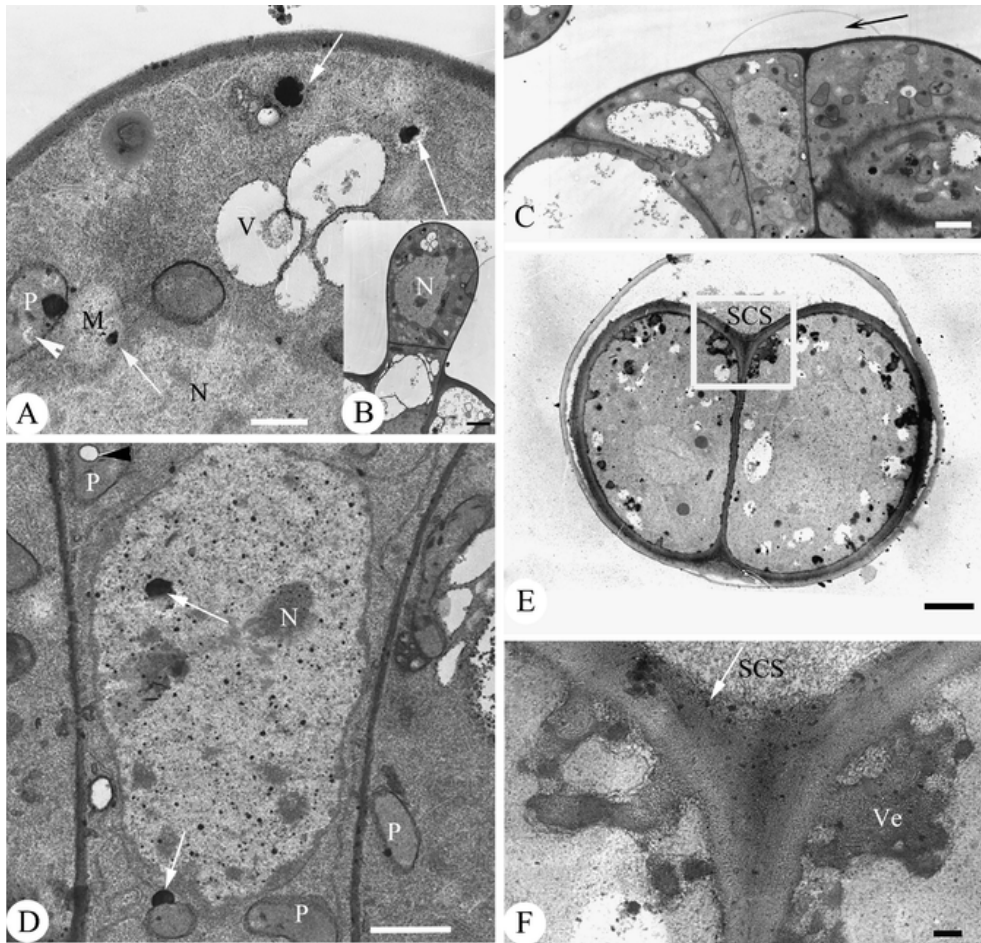
Fig. 2

TEM micrographs of *L. pinnata* glandular trichomes after 12-h HS. **a** Early presecretory stage of a gland initial cell tip (**b**), showing a few calcium ppts (*arrows*) in the mitochondria (*M*) and plastids (*P*). In some regions of the plastids the electron density is very low (*arrowhead*). *N* nucleus, *V* vacuole. *Bar* = 500 nm. **b** TEM of the whole presecretory gland, a detail of which is shown in **a**. *N* nucleus. *Bar* = 1 μm. **c** Peltate glandular trichome at the early secretory stage, showing the abnormal subcuticular space (SCS *arrow*). *Bar* = 2 μm. **d** Disk cells of a peltate glandular trichome at the early secretory stage, showing calcium ppts (*arrows*) deposited in the nucleus (*N*) and on the plastid (*P*) membranes. Some plastids contain vacuoles (*black arrowhead*). *Bar* = 1 μm. **e** Head of a capitate glandular trichome at the secretory stage, showing the abnormal *SCS*. *Box* enlarged portion of the cells shown in **f**. *Bar* = 2 μm. **f** Head cells of a capitate trichome enlarged from **e**, showing fusion of the secretory vesicles (*Ve*) with the plasma membrane. A few calcium ppts (*arrow*) appear on the border of the subcuticular space (*SCS*). *Bar* = 200 nm
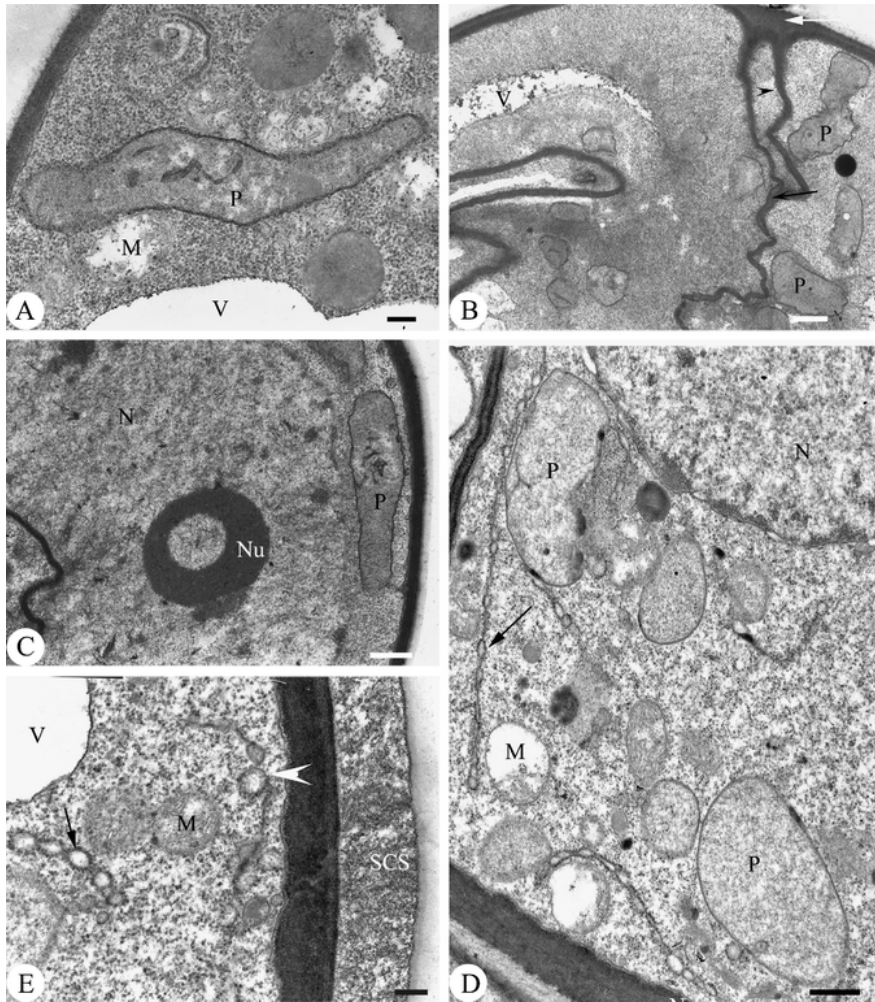
Fig. 3

TEM micrographs of peltate glandular trichomes after 48-h HS. Calcium ppts are absent from the gland cytosol and organelles. **a** Tip of a gland initial cell with plastids (*P*) lacking stroma and containing osmiophilic deposits. The mitochondria (*M*) lack
cristae. *V* vacuole. *Bar* = 200 nm. **b** Early secretory stage of a peltate trichome showing distortions in the cell wall (*black arrow*), plasma membrane (*arrowhead*), and plastid (*P*) membranes. No calcium ppts occur in the SCS (*white arrow*). *Bar* = 500 nm. **c** A disk cell of a peltate trichome at the secretory stage showing a ring-like nucleolus
(*Nu*). *N* nucleus, *P* plastids. *Bar* = 500 nm. **d**Peltate trichome disk cell at the secretory stage showing chain-like ER (*arrows*), vacuolated mitochondria (*M*), and plastids (*P*) with low electrical density. *N* nucleus. *Bar* = 500 nm. **e** Secretory stage of a peltate trichome disk cell with bulbous ER lamellae (*arrow*) with attached ribosomes. Some of the ER are represented by small, vesiculated remnants (*white arrowhead*). No calcium ppts occur in the subcuticular space
(*SCS*). *Bar* = 200 nm
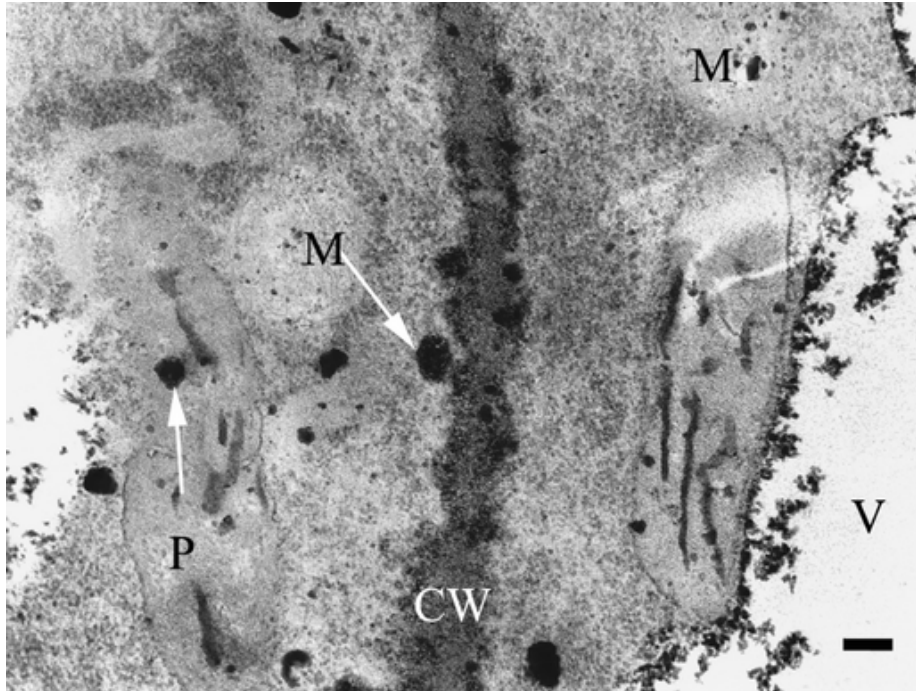
Fig. 4

TEM micrograph of peltate trichome head cells at the secretory stage, after recovery from 48-h HS. Calcium ppts (*arrows*) reappear in the disk cells. *CW* cell wall; *M* mitochondria; *P* plastid; *V* vacuole. *Bar* = 200 nm

Control: gland ultrastructure and calcium distribution during normal growth

This section is a summary of the results reported in Huang et al. (*2010*). Calcium precipitates are common at the beginning of gland development. Deposits are abundant in the cell wall; common in the nucleus, on the tonoplast and plasma membrane; and uncommon in the mitochondria, cytoplasmic matrix, and plastids (Huang et al. *2010*, their Fig. 1A). At the presecretory stage, calcium precipitates are commonly observed on the cell walls, plasma membrane, tonoplast, and in the nucleus and uncommon in the cytosol, mitochondria, and plastids (Huang et al. *2010*, their Fig. 2B). During the secretory stage, additional calcium precipitates appear in the SCS (Huang et al. *2010*, their Fig. 2F). During the post-secretory stage, as the organelles begin to degenerate, calcium precipitates reappear in the cytoplasm and organelles of all trichome cells, though they are most abundant in the apical cells. Calcium precipitates are absent from the SCS at this stage (Huang et al. *2010*, their Fig. 2H).

Control: treatment with Nif and EGTA

These results were first reported in Huang et al. (*2010*). Nif- and EGTA-treated plants show similar growth and ultrastructural defects in their trichomes. The effects are more extreme with increasing concentration of these chemicals. Symptoms include dry leaf margins, buds with tip

burn, the cessation of apical growth, and decreased glandular trichome density (Huang et al. *2010*).

The ultrastructural effects of Nif and EGTA treatments are similar in both types of trichomes. Following treatment, the cytoplasmic density of the cells decreases at all stages. At the early presecretory stage almost no calcium precipitates are observed in the gland initials following treatment (Huang et al. *2010*, their Fig. 4A). In a striking difference from untreated glands, parts of the cuticular layer separate from the cell wall at the presecretory stage to form an abnormal SCS (Huang et al. *2010*, their Fig. 4B). At the secretory stage, the vesicles are abnormal (Huang et al. *2010*, their Fig. 4C), and the SCS is nearly empty of secretory product (Huang et al. *2010*, their Fig. 4D). At the post-secretory stage, a few calcium precipitates appear on the membranes of the degenerating plastids, the cell walls acquire a lax fibrillar appearance (Huang et al.*2010*, their Fig. 4E), and the cuticular layer is thinner than in the controls (Huang et al. *2010*, their Fig. 4F).

Changes in glandular trichomes following HS

After 12-h HS, calcium ppts are much less abundant than in glands that have not been subjected to heat shock (Table 1, Fig. 1). At the initial and presecretory stages, calcium ppts are absent or uncommon from all subcellular structures and the cytosol (Table 1, Figs. 1 and 2a, b, arrows). At the early secretory stage, HS induces abnormal SCS formation (Fig. 2c, arrow). At the secretory stage, the only ppts that appear are in the plastids, SCS, on the plasma membrane (Table 1, Fig. 2d), and a few that occur in the secretory vesicles (Fig. 2f).

After 12-h HS, the early presecretory and secretory stage cells show symptoms of cellular injury (Fig. 2a–d). The plastids have a low electron density, lack stroma and osmiophilic deposits, and may even have electron lucent areas (Fig. 2a, d). During the secretory stage in capitate glandular trichomes, vesicles loaded with osmiophilic substance fuse together and adhere to the cell wall (Fig. 2e, f).

After 24-h HS, calcium ppts continue to decrease and almost completely disappear, except during the presecretory stage (Fig. 1). Additional ultrastructural damage occurs in both types of trichomes, though it is not described here.

In the remainder of this section, we will only describe the changes in the peltate trichomes. Both capitate and peltate trichomes responded to 48-h HS in similar ways, so describing the effects in both types would involve unnecessary repetition.

In response to 48-h HS, ppts disappear from all organelles and regions at all developmental stages (Fig. 3a–e), including from the SCS (Fig. 3b, white arrow). The cells also show many symptoms of cellular injury (Fig. 3a–e). The plastids are disorganized and vacuolated, and distinct cristae are no longer visible in the mitochondria (Fig. 3a). At the early secretory stage, the plasma and plastid membranes are distorted, and osmiophilic substances are nearly absent

from the plastids (Fig. 3b). The nucleus suffers from serious damage, including disruption of the nuclear envelope and condensation of the nucleoplasm (Fig. 3c). At the secretory stage, the cisternae of the ER are found around the periphery of the cell, are distended and chain-like, and are associated with prominent ribosomes (Fig. 3d, e), or leave small, vesiculated remnants (Fig. 3e, white arrowhead).

After 16 h of recovery at 24°C, a few calcium ppts reappear in the gland cells (Fig. 4). Some are located on the tonoplast and in the vacuole, in the plastids and cytosol, and on the plasma membrane (Fig. 4). A few also occur in the mitochondrial matrix.

Changes in mesophyll cells following HS

The spongy mesophyll cells from control plants contain large nuclei and vacuoles and have thylakoid membranes that are intact. The mitochondria also have intact membranes and cristae. Large (Fig. 5a, arrows) and small (Fig. 5a, arrowheads) calcium ppts are common in the nucleus, chloroplast (on the thylakoid membranes), and in the intercellular spaces. Participates are also common in the vessel elements (Fig. 5d). No ppts occur in the cytosol (Table 1, Fig. 5a).
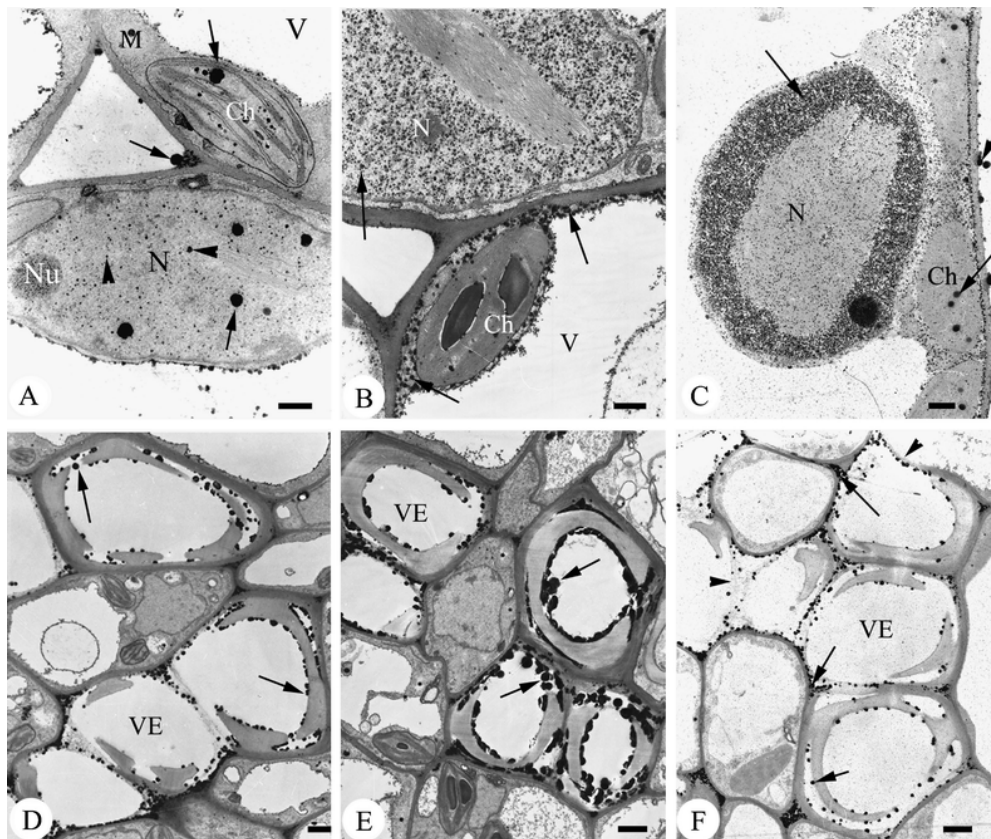
Fig. 5

TEM micrographs of mesophyll cells. **a** Mesophyll cells of the control (no HS). The organelles contain many big (*arrows*) and small (*arrowheads*) calcium ppts. Precipitates also occur on the

plasma membrane and tonoplast, are plentiful in the nucleus (*N*), and occur, though in lesser numbers, in the extracellular spaces and mitochondria (*M*). The chloroplast (*Ch*) thylakoid membranes are intact. *V* vacuole. *Bar* = 500 nm. **b** After 12-h HS, calcium deposits (*arrows*) increase in the nucleus, while decreasing in the vacuole (*V*). Many calcium ppts also appear for the first time in the cytosol. *Ch* chloroplast. *Bar* = 500 nm. **c** After 48-h HS, the calcium ppts (*arrows*) increase throughout the cell, and the organelles, except in the vacuole, where they decline slightly. The chloroplasts (*Ch*) and nucleus (*N*) degenerate. *Bar* = 500 nm. **d** Vascular bundle of the control, showing calcium distribution (*arrows*). *VE* vessel element. *Bar* = 1 μm. **e** Vascular bundle after 12-h HS, showing an increased number of calcium ppts (*arrows*) in the vessel elements (*VE*). *Bar* = 2 μm. **f**Vascular bundle after 48-h HS, showing a further increase in calcium ppts (*arrows*) in the vessel elements (*VE*), and the distortion of the vascular elements whose cell walls have degenerated (*arrowheads*). *Bar* = 1 μm

After 12-h HS, the structure of the cells and organelles are still relatively intact. Calcium ppts increase on the cell wall and in the nucleus, cytosol, and vessel elements (Table 1, Figs. 1 and 5b). Precipitates decrease on the tonoplast (Fig. 5b) and remain constant elsewhere. Compared to the control (Fig. 5d), many more calcium ppts occur in the vessel elements following 12-h HS (Table 1, Fig. 5e).

In response to 48-h HS, calcium ppts increase or remain at the same levels in all parts of the mesophyll cells, except on the tonoplast, where they decline slightly (Figs. 1 and 5c). They also decline in the intercellular spaces. Abundant calcium ppts are observed throughout the cytosol (Fig. 5c), and the number of participates continues to increase in the vessel elements (Fig. 5f). The organelles and nuclei degenerate during this time. In general, calcium ppts decrease in the gland cells in response to HS, while increasing in the mesophyll cells and vessel elements.

Discussion

Calcium available for binding by antimonate is termed "loosely bound" since only calcium present in more soluble compounds will release cationic calcium for antimonate precipitation. This loosely bound calcium may, under certain conditions, be mobilized and serve as a source of free Ca^{2+} (Tian et al. *2000*). Thus, calcium ions associated with allosteric compounds may be nearly as dynamic as calcium in the free cytosolic pool (Bush *1995*). Although the calcium susceptible to antimonate precipitation shares common solubility characteristics, the calcium thus visualized may have very different physiological functions in different cellular compartments (Boudsocq and Sheen *2010*).

Ca^{2+} is known to influence cell function through spatial and temporal changes in concentration induced by internal and external stimuli (Bush *1995*). For instance, intracellular Ca^{2+} levels often increase significantly under stress (Lynch et al. *1987*; Jian et al. *1999*; White *2001*). Ca^{2+} uptake has also been shown to be significantly enhanced by elevated temperature (Klein and Ferguson *1987*; Biyaseheva et al. *1993*; Gong et al. *1997*; Yan et al. *2002*).

The present study shows that changes in calcium distribution in glandular trichomes following HS occur in a regular sequence, but decrease instead of increasing as we originally hypothesized. Calcium ppts even disappear after 48-h HS. Calcium abundance is most strongly affected in the cytosol and tonoplast, followed by the cell wall, plasma membrane, and nucleus. The mitochondria and plastids are less strongly affected, but they also show fewer ppts before HS. In contrast, we found that calcium ppts increase in mesophyll cells and vessel elements following HS.

Since gland development is rapid (ca. 60 h from the initial cell to the mature trichome: Turner et al. *2000*), the secretory stage trichomes that received 48 h of HS experienced elevated temperatures during much of their development, while the initial and presecretory stage trichomes likely experienced elevated temperatures throughout their full development. The fact that no calcium ppts were found in any of these cells shows the severity of the effects of HS. Initial cells exposed to 12 h of HS have also likely been exposed for much of their development, while presecretory and secretory stage cells exposed to 12-h HS were exposed for proportionally less time. The fact that initial and presecretory stage cells show the same average number of ppts after 12-h HS (Fig. 1), while secretory cells show fewer ppts, suggests that the greatest sensitivity to HS occurs at the secretory stage of gland development. This conclusion is supported by the fact that abnormal SCS formation can occur at the early secretory stage after only 12-h HS.

Research on young leaves of heat-sensitive plants shows the same types of alterations in the ER (Pareek et al. *1997*), nucleus and nuclear membrane (Miao et al. *1994*; Ma et al. *2003*; Ruelland and Zachowski *2010*), and plasma membrane (Steponkus *1981*; Santarius and Weis *1988*; Pareek et al. *1997*) that we report here. The structure of HS gland cells is also similar to gland cells treated with the calcium blocker nifedipine (Huang et al. *2010*). Nifedipine-induced calcium deficiency is correlated with the premature formation of the SCS (Huang et al. *2010*), a condition that occurs in some peltate trichomes after 12 h of HS. Therefore, it is possible that the cellular responses reported here, including cellular degeneration, are partly mediated by calcium deficiency.

Prominent ER–ribosome complexes have been noted in response to water deficit, cold stress, and oxygen deficiency in other plant species. These changes may result from induction of stress proteins (Mistrik et al.*1992*; Ciamporova and Mistrik *1993*; Singla et al. *1997*). Similar changes have also been found in mesophyll cells in response to heat stress (Pareek, et al. *1997*). The change in ER morphology, with its increased association with ribosomes may enhance the synthesis of stress proteins from the lamellae which remain active (Pareek et al. *1997*).

Unlike the trichomes, and in accordance with our initial expectations, calcium abundance increases in the mesophyll cells following HS. This increase may be an adaptive response to HS. Several studies have shown that calcium is involved in plant tolerance to HS (Bramm *1992*; Biyaseheva et al. *1993*; Colorado et al. *1994*; Jiang and Huang *2001*; Liu et al. *2003*). Increasing

cytosolic [Ca^{2+}] following HS may alleviate heat injury and enable plant cells to better survive (Gong et al. *1998*; Wang and Li. *1999*; Liu et al. *2003*). Some of the best evidence for this comes from the induction of heat shock proteins (HSPs). An increase in cellular [Ca^{2+}] is involved in regulating the binding activity of the heat shock transcription factor to the HS element (Mosser et al. *1990*; Kuznetsov et al. *1998*; Trofimova et al. *1999*; Li et al. *2004*), the synthesis of HSPs (Kiang et al.*1994*; Kuznetsov et al. *1998*), and acquisition of HS-induced thermotolerance (Gong et al. *1997*; Kuznetsov et al. *1998*). The fact that the ability of plants to survive HS decreases with the addition of Ca^{2+} transport inhibitors supports a role for calcium in protecting against HS (Gong et al. *1997*; Zhang et al. *2000*).

If a high [Ca^{2+}] provides protection from HS, excessive Ca^{2+} can be cytotoxic (Hepler and Wayne *1985*; Minorsky *1985*; Biyaseheva et al. *1993*; Bush *1995*; Clapham *1995*; Jian et al. *1999*; Wang and Li *1999*). The cellular changes we observed in the mesophyll cells and vessel elements after 48-h HS may be due to heat stress-induced high levels of Ca^{2+} in these cells. In contrast, the slightly less damage to the gland cells may be due to low calcium abundance in these cells.

Ca^{2+} uptake has been shown to be significantly enhanced under HS, with the increased Ca^{2+} mainly acquired from the growth medium via the xylem (Canny *1990*; Leigh and Tomos *1993*; Karley et al. *2000*; White *2001*). In our study, increasing exposure to HS leads to an increasing number of calcium ppts being deposited in the vessel elements. This finding is consistent with the hypothesis that Ca^{2+} enters the leaves via the xylem. However, with increasing HS the amount of Ca^{2+} in the trichomes (as measured by the number of ppts) declines. Where does this Ca^{2+} go? It may be possible that some of the Ca^{2+} in the mesophyll cells comes from the trichomes via intercellular transport, though additional tests would be necessary to substantiate this hypothesis.

Supporting this hypothesis, it has been found that trichomes play an important role in regulating the amount of calcium in the leaf in *Centaurea scabiosa* and *Leontodon hispidus* (both Asteraceae). In these species, calcium is strongly concentrated in the trichomes, which protects the guard cells from the high calcium concentrations delivered in the transpiration stream (De Silva et al. *1996*). That calcium ppts appear again in the trichomes during recovery from the HS in *Lavandula* also suggests that Ca^{2+} may flux to the places where it is needed most. In order to tolerate HS, Ca^{2+}may not only be taken up from the transpiration stream, but may be transported from the trichomes, and perhaps from other epidermal cells. In order to test this hypothesis it would, at a minimum, be necessary to show that the addition of exogenous Ca^{2+} can rescue the trichomes from heat shock.

Conclusion

Calcium is an important mediator of HS (Boudsocq and Sheen *2010*). Calcium levels decrease in *Lavandula*trichomes following HS, while increasing in the mesophyll cells and vessel

elements. Prolonged exposure to decreased calcium levels is correlated with degeneration of the organelles, and a breakdown of intercellular structure (Burstrom *1968*; Huang et al. *2010*), while elevated levels, if moderate, provide some protection from HS (Gong et al. *1998*; Wang and Li. *1999*; Liu et al. *2003*). Decreased calcium levels, whether artificially induced (Huang et al. *2010*), or resulting from HS (this study), are expected to lead to a reduction in essential oil production, as most organelles that participate in the synthesis and transport of essential oils are damaged at low calcium levels. The uneven calcium distribution observed in the gland and mesophyll cells of *Lavandula* may partially result from calcium flux between these locations. Calcium may be redistributed from less (trichomes) to more (mesophyll) essential parts of the leaf.

Acknowledgments

References

Abdelmageed AHA, Grudaz N (2007) Influence of heat shock pretreatment on growth and development of tomatoes under controlled heat stress conditions. J Appl Bot Food Qual 81:26–28

Amelunxen F, Gronau G (1968) Elektronenmikroskopische untersuchungen an den Olzellen von *Acorus calamus* L. Z Pflanzenphysiol 60:156–168

Antunes T, Sevinate-Pinto I (1991) Glandular trichomes of *Teucrium scorodonia* L. morphology and histochemistry. Flora 185:65–70

Biyaseheva AE, Molotkovskii YG, Mamonov LK (1993) Increase of free Ca^{2+} in the cytosol of plant protoplasts in response to heat stress as related to Ca^{2+} homeostasis. Russian J Plant Physiol 40:540–544

Blum A (1996) Plant breeding for stress environments. CRC, Boca Raton

Burstrom HG (1968) Calcium and plant growth. Bio Rev 43:287–316

Boudsocq M, Sheen J (2010) Stress signaling II: calcium sensing and signaling. In: Pareek A, Sopory SK, Bohnert HJ, Govindjee (eds) Abiotic stress adaptation in plants: physiological, molecular and genomic foundation. Springer, Dordrecht, pp 75–90

Boursiac Y, Lee SM, Romanowsky S, Blank R, Sladek C, Chung WS, Harper JF (2010) Disruption of the vacuolar calcium-ATPases in *Arabidopsis*results in the activation of a salicylic acid-dependent programmed cell death pathway. Plant Physiol 154:1158–1171

Bramm J (1992) Regulated expression of the calmodulin-related TCH genes in cultured *Arabidopsis* cells: induction by calcium and heat shock. Proc Natl Acad Sci USA 89:3213–3216

Bush DS (1995) Calcium regulation in plants cells and its role in signaling. Annu Rev Plant Physiol Plant Mol Biol 46:95–122

Canny MJ (1990) What becomes of the transpiration stream? New Phytol 114:341–368

Ciamporova M, Mistrik I (1993) The ultrastructural response of root cells to stressful conditions. Environ Exp Bot 33:11–26

Clapham DE (1995) Calcium signaling. Cell 80:259–268

Collins GG, Nie XL, Saltveit ME (1995) Heat-shock proteins and chilling sensitivity of mung bean hypocotyls. J Exp Bot 46:795–802

Colorado P, Rodriguez A, Nicolas G, Rodriguez D (1994) Abscisic acid and stress regulate gene expression during germination of chick-pea seeds. Possible role of calcium. Physiol Plantarum 91:461–467

De Silva DLR, Hetheringtion AM, Mansfield TA (1996) Where does all the calcium go? Evidence of an important regulatory role for trichomes in two calcicoles. Plant Cell Environ 19:880–886

Gersbach PV (2002) The essential oil secretory structures of *Prostanthera ovalifolia* (Lamiaceae). Ann Bot 89:255–260

Gilroy S, Read ND, Trewavas AJ (1990) Elevation of cytoplasmic calcium by caged calcium or caged inositol triphosphate initiates stomatal closure. Nature 346:769–771

Gong M, Li YJ, Dai X, Tian M, Li ZG (1997) Involvement of calcium and calmodulin in the acquisition of heat-shock induced thermotolerance in maize. J Plant Physiol 150:615–621

Gong M, van der Luit AH, Knight MR, Trewavas AJ (1998) Heat-shock-induced changes in intracellular Ca^{2+} level in tobacco seedlings in relation to thermotolerance. Plant Physiol 116:429–437

Hepler PK, Wayne RO (1985) Calcium and plant development. Ann Rev Plant Physiol 36:397–439

Huang SS, Kirchoff BK, Liao JP (2008) The capitate and peltate glandular trichomes of *Lavandula pinnata* L. (Lamiaceae): histochemistry, ultrastructure and secretion. J Torrey Bot Soc 135:155–167

Huang SS, Liao JP, Kirchoff BK (2010) Calcium distribution and function in glandular trichomes of *Lavandula pinnata* L. (Lamiaceae). J Torrey Bot Soc 137:1–15

Jian LC, Li JH, Chen WP, Paul HL, Ahlstrand GG (1999) Cytochemical localization of calcium and Ca^{2+}-ATPase activity in plant cells under chilling stress: a comparative study between the chilling-sensitive maize and the chilling-insensitive winter wheat. Plant Cell Physiol 40:1061–1071

Jiang YW, Huang BG (2001) Effects of calcium on antioxidant activities and water relations associated with heat tolerance in two cool-season grasses. J Exp Bot 52:341–349

Karley AJ, Leigh RA, Sanders D (2000) Where do all the ions go? The cellular basis of differential ion accumulation in leaf cells. Trends Plant Sci 5:465–470

Kiang JG, Carr FE, Burns MR, McClain DE (1994) HSP-72 synthesis is promoted by increase in $[Ca^{2+}]_i$ or activation of G proteins but not pHi or cAMP. Am J Physiol–Cell Physiol 267:104–114

Klein JD, Ferguson IB (1987) Effect of high temperature on calcium uptake by suspension-cultured pear fruit cells. Plant Physiol 84:153–156

Knight MR, Campbell AK, Smith SM, Trewavas AJ (1991) Transgenic plant aequorin reports the effects of touch and cold-shock and elicitors on cytoplasmic calcium. Nature 352:524–526

Kuznetsov VV, Andreev IM, Trofimova MS (1998) The synthesis of HSPs in sugar beet suspension culture cells under hyperthermia exhibits differential sensitivity to calcium. Biochem Mol Biol Int 45:269–278

Leigh RA, Tomos AD (1993) Ion distribution in cereal leaves: pathways and mechanisms. Philos Trans Royal Soc Lond B Biol Sci 341:75–86

Li B, Liu HT, Sun DY, Zhou RG (2004) Ca^{2+} and calmodulin modulate DNA-binding activity of maize heat shock transcription factor in vitro. Plant cell Physiol 45:627–634

Liu HT, Li B, Shang ZL, Li XZ, Mu RL, Sun DY, Zhou RG (2003) Calmodulin is involved in heat shock signal transduction in wheat. Plant Physiol 132:1186–1195

Lynch DV, Lepock JR, Thompson JE (1987) Temperature-induced changes in lipid fluidity alter the conformation of proteins in senescing plant membranes. Plant cell Physiol 28:787–797

Ma XD, Wang L, Wang M, Peng H (2003) Difference in relative conductivity and ultrastructure of leaf between two wheat cultivars with different thermotolerance under heat acclimation and heat stress. Journal of China Agricultural University 8:4–8 (in Chinese)

Miao C, Li RQ, Wang JB (1994) Ultrastructural study in leaf cell of *Brassica oleracea* var. *capitata* under heat stress. Acta Bot Sinica 36:730–732, in Chinese

Minorsky PV (1985) A heuritic hypothesis of chilling injury in plants: a role for calcium as primary physiological transducer of injury. Plant Cell Environ 8:75–94

Mistrik M, Holobrada M, Ciapporova M (1992) The root in unfavourable conditions. In: Kolek J, Kozinka V (eds) Physiology of plant root system. Kluwer Academic, Dordrecht, pp 286–312

Mosser DD, Kotzbauer PT, Sarge KD, Morimoto RI (1990) In vitro activation of heat shock transcription factor DNA-binding by calcium and biochemical conditions that affect protein conformation. Proc Natl Acad Sci U S A 87:3748–3752

Nicotera P, Zhivotovsky B, Orrenius S (1994) Nuclear calcium transport and the role of calcium in apoptosis. Cell Calcium 16:279–288

Palta JP (1990) Stress interactions at the cellular and membrane levels. Hortic science 25:1377–1381

Pareek A, Singla S, Grover A (1997) Short-term salinity and high temperature stress-associated ultrastructural alterations in young leaf cells of *Oryza sativa* L. Ann Bot 80:629–639

Ruelland E, Zachowski A (2010) How plants sense temperature. Enviro Exp Bot 69:225–232

Santarius KA, Weis E (1988) Heat stress and membranes. In: Plant membranes—structure, assembly and function. Biochem Soc, pp 97-112

Simon EW (1978) The symptoms of calcium deficiency in plants. New Phytology 80:1–15

Singla SL, Pareek A, Grover A (1997) High temperature. In: Prasad MNV (ed) Plant ecophysiology. Wiley, New York, pp 101–127

Slocum RD, Roux SJ (1982) An improved method for the subcellular localization of calcium using a modification of the antimonate precipitates technique. J Histochem Cytochem 30:617–629

Starck Z, Siwiec A, Chotuj D (1994) Distribution of calcium in tomato plants in response to heat stress and plant growth regulators. Plant Soil 167:143–148

Steponkus PL (1981) Responses to extreme temperatures: cellular and sub-cellular bases. In: Lange OL, Nobel PS, Osmond CB, Ziegier H (ed) Physiological plant ecology: responses to the physical environment. Springer, New York, 12: 372-402

Tian HQ, Russell SD (1997) Calcium distribution in fertilized and unfertilized ovules and embryo sacs of *Nicotiana tabacum* L. Planta 202:93–105

Tian HQ, Zhu H, Russell SD (2000) Calcium changes in ovules and embryo sacs of *Plumbago zeylanica* L. Sex Plant Rep 13:11–20

Trofimova MS, Andreev IM, Kuznetsov VV (1999) Calcium is involved in regulation of the synthesis of HSPs in suspension-cultured sugar beet cells under hyperthermia. Physiol Plant 105:67–73

Turner GW, Gershenzon J, Croteau RB (2000) Development of peltate glandular trichomes of peppermint. Plant Physiol 124:665–680

Vierling E (1991) The roles of heat shock proteins in plants. Ann Rev Plant Physiol Plant Mol Biol 42:579–602

Wang GY, Liu JM, Zhang Y, Yu BS, Shen ZY (1997) Studies on ultrastructure in common bean leaves during heat acclimation and heat stress. J Agric Biotech 7:151–156 (in Chinese)

Wang JB, Li RQ (1999) Changes of Ca^{2+} distribution in mesophyll cells of pepper under heat stress. Acta Hortic Sinca 26:57–58

Wahid A, Gelani S, Ashraf M, Foolad MR (2007) Heat tolerance in plants: an overview. Environ Exp Bot 61:199–223

Webb AAR, Mcainsh MR, Taylor JE, Hetherington AM (1996) Calcium ions as intracellular second messenger in higher plants. Adv Bot Res 22:45–96

Werker E (1993) Function of essential oil-secreting glandular hairs in aromatic plants of the Lamiaceae—a review. Flavor Fragr J 8:249–255

White PJ (2001) The pathways of calcium movement to the xylem. J Exp Bot 52:891–899

Wick SM, Hepler PK (1980) Localization of Ca^{2+}-containing antimonate precipitations during mitosis. J Cell Biol 86:500–513

Yan CL, Wang JB, Li RQ (2002) Effect of heat stress on calcium ultrastructural distribution in pepper anther. Environ Exp Bot 48:161–168

Zhang ZS, Li RQ, Wang JB (2000) Effect of Ca^{2+}, La^{3+} and EGTA treatment on the responses of pepper leaves to heat stress. J Wuhan Univ 46:253–256 (in Chinese)

Zhao HJ, Tan JF (2005) Role of calcium ion in protection against heat and high irradiance stress-induced oxidative damage to photosynthesis of wheat leaves. Photosynthetica 43:473–476.